Prototyping and control of a robotic gripper

Yago Felipe de Moura - 42825

Thesis presented to the Superior School of Technology and Management (ESTiG) as part of a Double Degree Program with the Federal University of Technology – Paraná (UTFPR) for obtaining the Master's Degree in Industrial Engineering.

Dissertation supervised by:

Prof. Dr. José Gonçalves

Prof. Dr. João Ribeiro

Prof. Dr. Winderson dos Santos

Bragança

2019-2020

Prototyping and control of a robotic gripper

Yago Felipe de Moura - 42825

Thesis presented to the Superior School of Technology and Management (ESTiG) as part of a Double Degree Program with the Federal University of Technology – Paraná (UTFPR) for obtaining the Master's Degree in Industrial Engineering.

Dissertation supervised by:

Prof. Dr. José Gonçalves

Prof. Dr. João Ribeiro

Prof. Dr. Winderson dos Santos

Bragança

2019-2020

Acknowledgement

I'd like to express my deepest thanks to my family.

Mom, Dad, thank you. Despite all the best education you've provided me, there hasn't been any lesson more important than the ones you've taught me.

Natalia, if it wasn't for you, I wouldn't even be writing this acknowledgement. Thank you for encouraging me to always do my best and for all the support throughout the process. You are amazing.

Felipe, thank you for all the afternoons spent discussing the study and laughing about it. From inexplicable events to miraculous recoveries, it's been a crazy period.

I also thank the professors involved in both supervising and evaluating this study for the guidance, patience and support.

Abstract

This paper consists on the design and modelling of a electric-actuated gripper structure, the production and assembly of a prototype with the use of a 3D printer and the development of an control system that limits the force applied by the tool. The final result, despite the motor limitation, allowed a study of the applied force control by manipulating a servo motor positioning.

Keywords: Gripper, Load cell, Servo motor, SolidWorks, LabVIEW.

Contents

List of Figures

Chapter 1

Introduction

Industrial robots are spread throughout many different activities on a production plant. From manipulating pieces, assembling, welding, painting to moving and storing materials and products. For every implementation there are different end effectors to fulfill it's purpose, those are the devices designed to interact with the environment. This thesis will study one of those end effectors, the gripper.

Used in many applications, there are just as many different pre-existing models. Nevertheless, on a market that has an increasing demand for personalized products, grippers are not an exception. Studies are constantly being made for new uses of grasping solutions.

1.1   Scope

The thesis is limited to the mechanical design and control system of servo-electric gripper. It does not cover the study of forces actuating on the gripper, such as shearing and torsional stresses.

1.2   Objectives

The objectives of this study are the design and modelling of a gripper with the software SolidWorks, the production and assembly of a prototype with the use of a 3D printer and

the development of an control system that limits the force applied by the tool. For this study, the following specification were defined:

- The gripper should have electric actuation;

- The final force applied by the tool on the grasped object must be controlled and limited;

- The end-effector is designed for grasping objects with a maximum force of 0.5kgf;

- The prototype is designed for a study environment.

1.3 Document Structure

This document is arranged in 6 chapters. Chapter 1 introduces the theme of the study, as well as scope and objectives. Chapter 2 brings a review of the evolution of grasping tools up to it's state-of-the-art applications. Chapter 3 includes the design and modelling of the end-effector, as well as a brief motion study using the software SolidWorks. Chapter 4 is about the printing and assembly of the model, with it's implementation, and the development of the control system. Chapter 5 covers the tests made and the evaluation of the performance of the prototype compared to the objectives previously stated. Finally, chapter 6 presents the conclusion and proposition of future studies.

Chapter 2

Gripper's State of the Art

Mankind has, since the early beginning of technique, used grasping tools in order to facilitate and/or make possible the manipulation of materials. As mentioned by M. Ceccarelli on [1], "Grasping tools were conceived and developed since Prehistory Times with the aim to help humans to grasp objects that were difficult for size, shape, materials, and conditions".

The first devices had a simple design, with two fingers and one joint, such as pliers, that allowed blacksmiths to safely work with high temperature materials. It was on early Renaissance, though, that more complex and specific devices started to be developed. On Figure 2.1 solutions for grasping and handling heavy loads are presented. Still on Figure 2.1, designs meant to safely handle living animals, and mechanisms to regulate the opening and grasping force of the gripper can be seen.

With the nineteenth century, solutions focused on improving the actuation power efficiency and studies on the mechanisms of grasp started to emerge. As stated on [1], "From simple mechanisms in early grippers at Renaissance, the functioning of grippers has required more efficient (complex) mechanisms that have been proposed mainly for industry applications in the nineteenth century and in modern time within a mechatronic design".

The introduction of industrial robotic brought a new era of gripper applications.
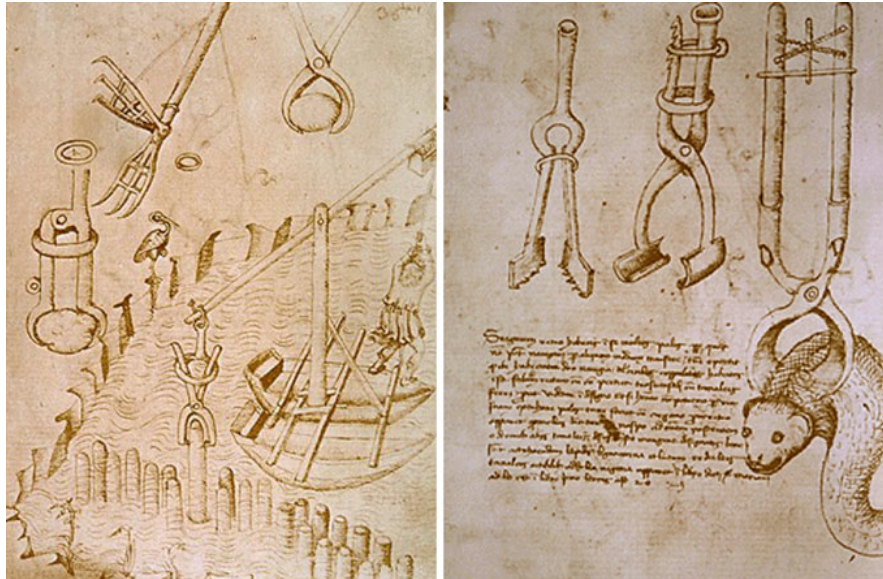
Figure 2.1: Mechanisms for grippers by Mariano di Jacopo (il Taccola) (1382-1458?) [1]

Robots were now taking over repetitive manufacturing operations that were before performed by humans, therefore, new studies had to be done on grasping techniques to fulfill the new range of operation needs. Nevertheless, the design with two fingers is still one of the most used on modern applications, both for simplicity and efficiency.

> "According to statistical studies, from 60 to 70% of man's grasping of objects of cylindrical, parallelepiped, and pyramidal shapes is performed with only two fingers. This is why two-finger grasp is well spread in the industrial applications and mainly in automated assembly." [2, page 107]

Modern manufacturing is filled with pick and place operations done by robots, from assembling automotive components to organizing electronic printed circuits and palletizing products. A quick look on a gripper catalogue shows a great variety of models for the conventional day-to-day industrial applications. Figure 2.2 presents some of the parallel grippers from company *Schunk*.

Although grippers have default models for most industrial basic needs, more specific applications that can not be executed with the classical models continue to appear. To

Co-act EGL-C
Collaborating long-stroke gripper
→ 0 Variants available

Co-act EGP-C
Collaborating gripper for small components
→ 16 Variants available

EGP
Gripper for small components

EGA
Long-stroke gripper

Figure 2.2: Models found on *https://schunk.com/*

attend their demand, new designs have to be developed according to the tasks characteristics.

An example of those applications is on marine life exploration, a research published on the journal *Science Robotics* presents a specially designed soft gripper able of manipulating fragile soft-bodied sea organisms, such as jellyfish. The study of what the article refers as "forgotten fauna", the gelatinous zooplankton, has a vast potential of discoveries on many different areas such as "materials and structures, cutting-edge medical treatments, and biomimetic manipulators and locomotors." [3]

> "Despite this vast potential, collecting intact samples of gelatinous organisms to study remains extremely challenging." "...existing technologies (e.g., nets and vacuum devices) frequently damage samples during the collection process." [3]

The authors utilized a silicone matrix and a strain-limiting layer of flexible polymer nanofibers to produce the actuator "fingers" attached to a 3D–printed "palm", composed

of a transparent photopolymer, produced using a PolyJet-based printer. The positioning of the actuators are arranged so they "overlap and contact one another, forming a soft network that restricts the position of the target but does not fully immobilize it; this caging grasp reduces the need to precisely control individual finger placement and instead relies on collective inflation of all actuators." [3]. During the experiments, the authors confirmed that, at the typical operating pressure of 6psi, the actuators applied an average contact pressure of 0.0455 ± 0.007 kPa, fulfilling the target of being bellow 1 kPa and ensuring a delicate grasp of soft-bodied organisms. Figure 2.3 represents the successful grasp of a jellyfish.
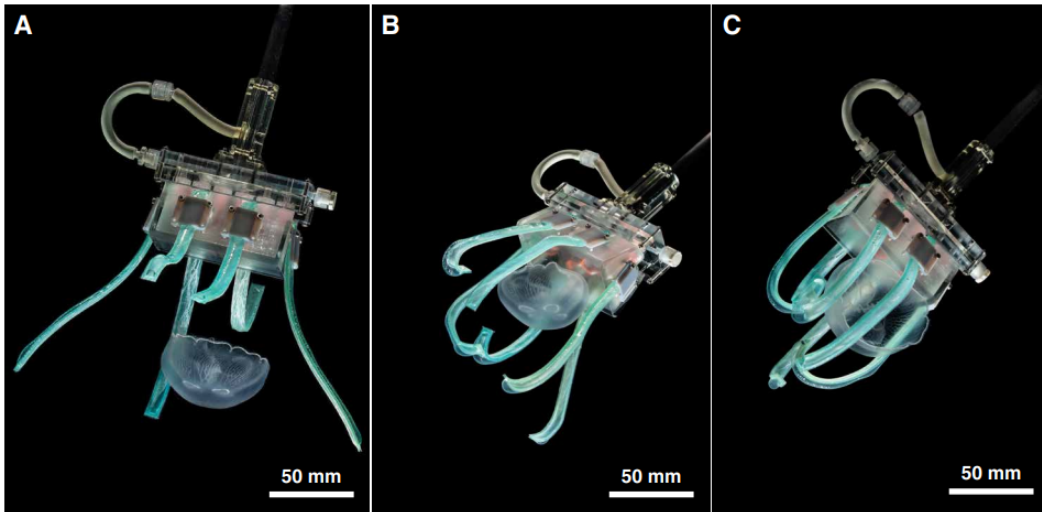
Figure 2.3: "**Gentle grasping of A. *aurita*. (A)** Actuators approach the jellyfish, uninflated. **(B)** Actuators begin to hydraulically pressurize. **(C)** Actuator pressurization continues until the jellyfish is gently and securely grasped. Photos courtesy of Anand Varma." [3]

In order to design a gripper, a series of items must be taken in account, such as the manipulated object's geometrical and physical characteristics, the operation to be executed and it's specifications, and the environment on which the task will occur. Information such as size and shape of the object define the size and grasp of the tool, as gravity center and object weight provides data about the optimal contact point and the necessary grasping force to safely manipulate the object. Another property analysed is the friction coefficient that, along with the weight and gravity center, determines how much strength

the gripper should apply. Figure 2.4 presents some topics evaluated during the project of a gripper.
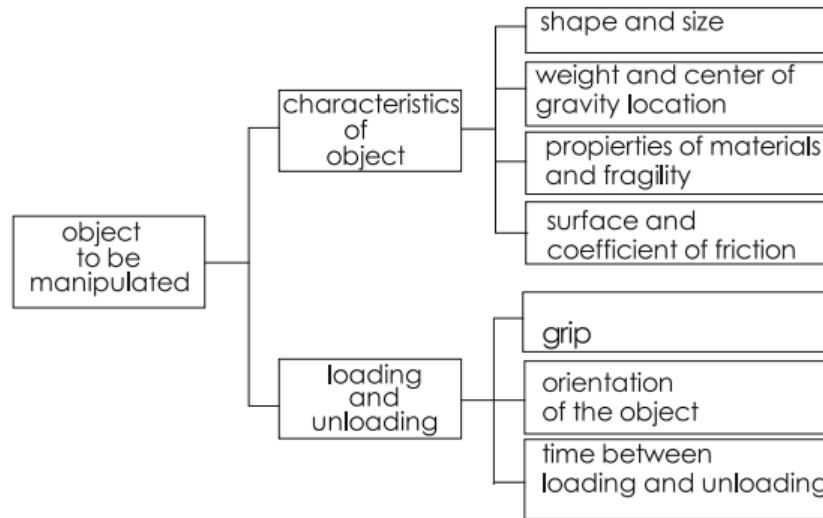
Figure 2.4: Characteristics of the object to be manipulated [2]

The keywords surrounding the newest trends on grippers are "soft grippers" and "adaptive grippers". Soft gripper is a concept regarding the effect the grasp will cause onto the held object. This is specially applied in food and health industries, where the materials are sensitive and, for example, easily deformed.

The soft kinematics found on the human hand have been recreated on soft grippers with many different techniques such as "multi material 3D printing, soft lithography, shape deposition manufacturing, and integrated multiple manufacturing approaches to create composite materials" [4]. Most solutions are produced with silicone rubber for it's flexibility and resilience.

A research published at *The International Conference on Robotics and Biomimetics* in 2018 uses natural rubber into the fabrication of a 4 finger soft gripper. The "Gripper consists of a rigid base and four soft actuators. Each soft actuator has four separate chambers inflated using compressed air" [4]. It has a simple ON/OFF actuation control and a bending angle feedback provided by a flex sensor embedded in the actuators. Figure 2.5 presents the successful lifts of different objects during the experiment.

Figure 2.5: Grasping and lifting operations (a) Grasping a cupcake by inflating inwards (b) Grasping a tomato (c) Grasping a raw egg (d) Lifting experiment [4]

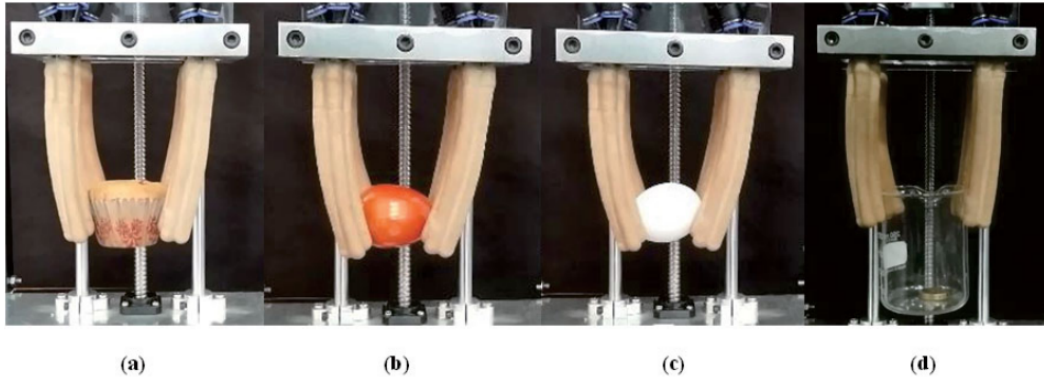Adaptive grippers are associated to the grasp of objects with non-regular shapes. The main idea is that the gripper has not only one grasp form, but instead can adapt it's shape as it grasps the object. Once again, a concept abstracted from the human hand.

About this concept, two examples will be shown. One is a adaptive gripper with independent finger joints [5] where the gripper digits conform to the shape of the object. The second one is a study of a gripper finger that is embedded with both, soft and adaptive concepts, utilizing shape memory alloys and tactile sensors [6].

The paper presented on the *2019 IEEE 15th International Conference on Automation Science and Engineering (CASE), "A Joint-Selective Robotic Gripper with Actuation Mode Switching"* [5], presents a dual mode gripper, capable of conforming to the shape of the objects with it's finger joints and, equipped with an individual joint lock system, safely handling the object with precision.

As stated on [5], gripper designers are constantly dealing with a trade-off between dexterity and grasping force, and the compactness and weight of the control unit and gripper. In order to achieve the dexterity required on the project, the authors chose to design a fully actuated system, which implies in matching the number of actuators (Degree of Actuation - DOA) with the number of degrees of freedom (DOF). Another requirement of the project was the actuation transmission via tendons.

"A high actuator force is associated with the disadvantage of a lack of

8

compactness and high weight due to the limited energy density attainable."
"Strong and dexterous robotic grippers, as in the case of the Shadow Hand with pneumatic actuators, typically includes the use of a large control unit."
[5]

The solution found for reducing the number of actuators was the use of electromagnetic individual joint locks. That way, each individual joint could be controlled by locking all others. "If all but one joint is locked, the movement can only be transferred to the unlocked joint. This corresponds to the possibility of the active control of any joint, i.e. a full actuation." [5]. Also, mechanical spring components were used in order to stretch the finger, so that no tendon control and extra actuator was necessary. Figure 2.6 represents the concept design of the finger, with the electromagnetic locking and the tendon transmission.
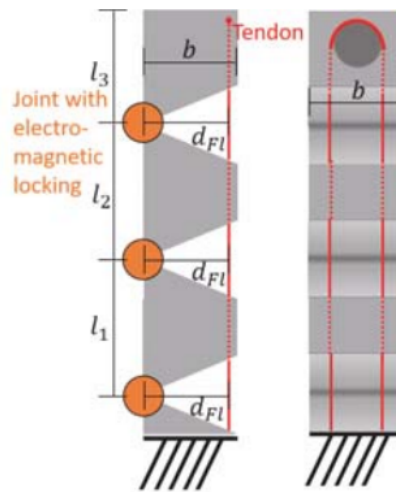
Figure 2.6: Schematic concept of the finger: model of the finger implementing the electromagnets mechanism [5]

As stated on [5], "The basic design principle of locking by means of electromagnets results in several decisive advantages.(...) With the electromagnets the system can be fully actuated which allows a high dexterity. Nevertheless, the complexity of the control itself is only slightly higher than that of underactuated systems (...). In addition, the design represents a more general solution for the compromise between size and weight,

and force and dexterity.". Figure 2.7 represents some of the results of the individual joint control.

Figure 2.7: Successful results of individual joint control [5]

The study "Novel Smart and Compliant Robotic Gripper: Design, Modelling, Experiments and Control" [6] presents the concept of a two-finger gripper and a functional prototype of one gripper finger using a shape memory alloy wire as actuator and conductive graphite foam for sensors.

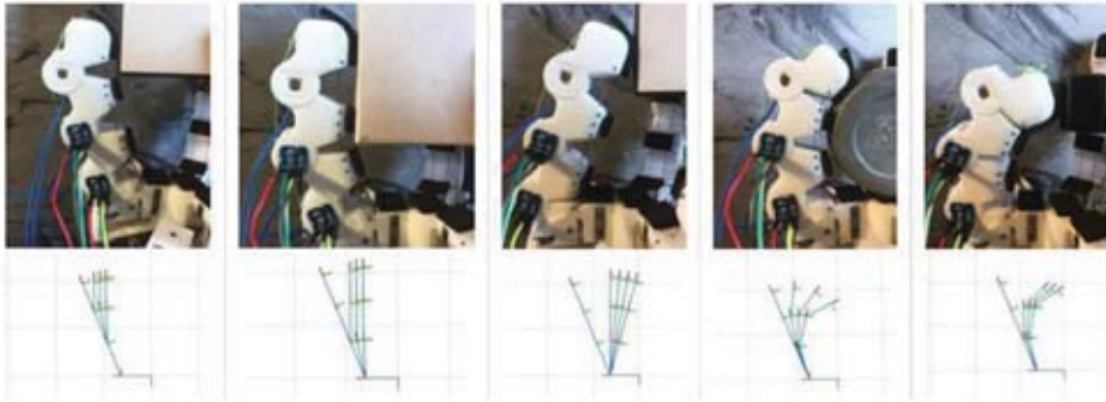> "Adaptive gripper proposed here is based on elastic active compliant mechanisms. Via integrated sensors, and actuators active smart gripper changes the shape of its grasping surface and adapts to the object of unknown shape."
>
> [6]

Unlike the previous example, this paper presents "a novel concept of the adaptive soft robotic gripper" [6]. The mechanism proposed deforms as one whole flexible monolithic structure in order to realize force and motion transmission, "... thus providing one unique advantage for achieving shape morphing and adaptability" [6]. Figure 2.8 presents a concept of a compliant system with actuators and sensors as a robotic two-fingered gripper.

As a result of the authors study, a prototype model of the two-fingered gripper was designed. Experiments with the designed model were made in order to the understand the behavior of the gripper with different combinations of contracting and expanding the actuators, as can be seen on Figure 2.9.
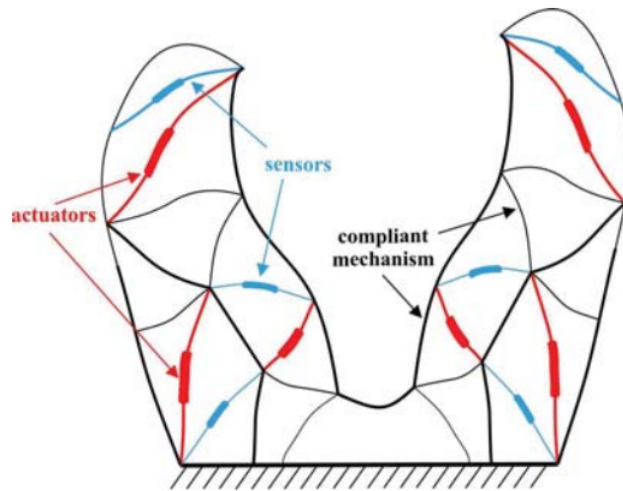
Figure 2.8: Illustration of a compliant system (compliant mechanisms with integrated sensors and actuators) as an adaptive soft robotic gripper [6]
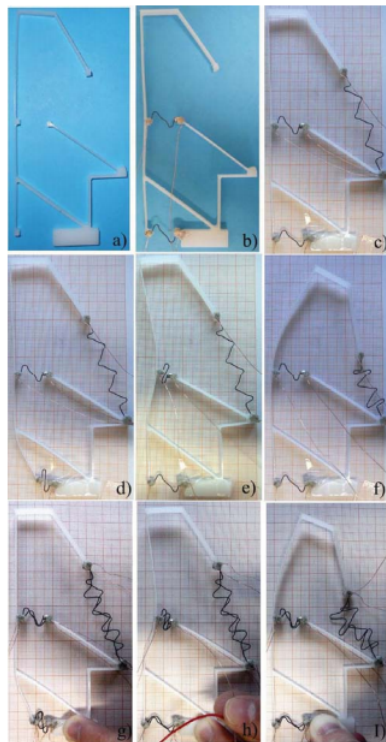

Figure 2.9: Results of the two-fingered behavior to different actuation combinations [6]

In order to incorporate sensors into the gripper, the authors chose to use graphite foam with copper wires to detect resistance differences on the foam as it deforms. Because of the non-linear behavior of the the displacement-electrical resistance characteristic, an Artificial Neural Network training was required to associate the graphite foam deformation and the voltage difference input. With the training completed, the foam was embedded into the gripper finger, making it possible to detect contact to grasped object, therefore enabling better conformation. The final gripper finger prototype can be seen on Figure 2.10. As future work, authors suggest assembling the two-fingered gripper as well as a more complex control of the actuator.
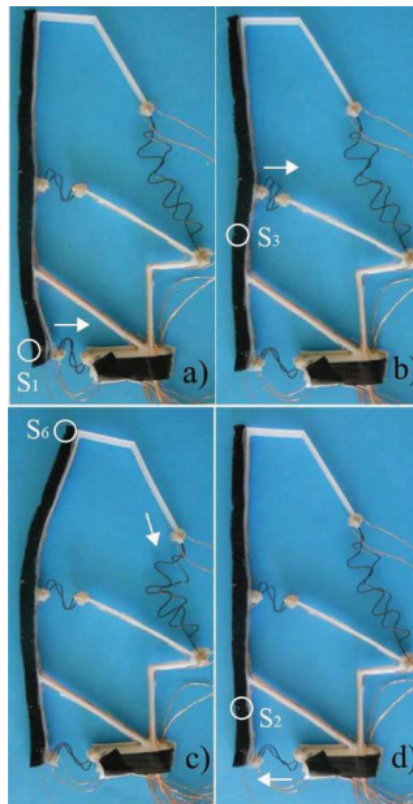
Figure 2.10: "Behavior of gripper finger with integrated nitinol actuators, foam sensors and control algorithm: a) activation of contracting actuator 1 by detecting contact in point S1; b) activation of actuator 2 by detecting contact in point S3; c) activation of actuator 3 by detecting contact in point S6; d) activation of expanding actuator 1b, by detecting contact in point S2." [6]

This chapter was a brief introduction to the vast gripper subjects found in literature.

From historical grasping objects to state-of-the-art soft adaptive grippers, the presence of such a tool in our lives is undeniable. Therefore, it's study is unavoidable.

Chapter 3

Mechanical Study

As presented on the last chapter, designing an end-effector involves analysing the characteristics needed for the project. For this study, the following specification were defined: The gripper should have electric actuation; The final force applied by the tool on the grasped object must be controlled and limited; The end-effector is designed for grasping objects with a maximum force of 0.5kgf; The prototype is designed for a study environment.

Once the characteristics were defined, the next step was implementing a design on the CAD software SolidWorks. Taking advantage of the software's vast user-made library, a pre-model was downloaded from *grabcad.com* and used as base, as shown on figure 3.1.

Upon this, several changes were made in order to fulfill the project's specifications. The fingers structures were adapted so the load cells could be fixed and used as contact point for grasping. The load cells chosen for the project had a 500g capacity each. The load cells were modelled on SolidWorks with the measured dimensions of the real model. For fixation, a two bolts and nuts set was used on each finger structure, figure 3.2. The gear set, along with the rods that sustain the finger structure, were redesigned for easier production with an 3d printer, figure 3.3. The transmission system and top plate were also updated accordingly to fit the servo motor, figure 3.4.

Once the design of all the parts was finished, a new assembly project was made, using Mates to simulate the coupling of the parts. The mates used were Coincident, Concentric
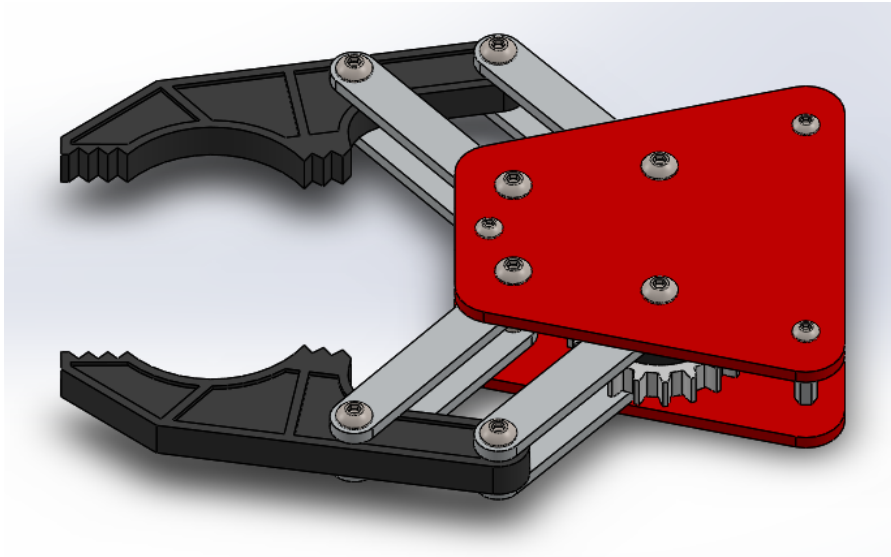
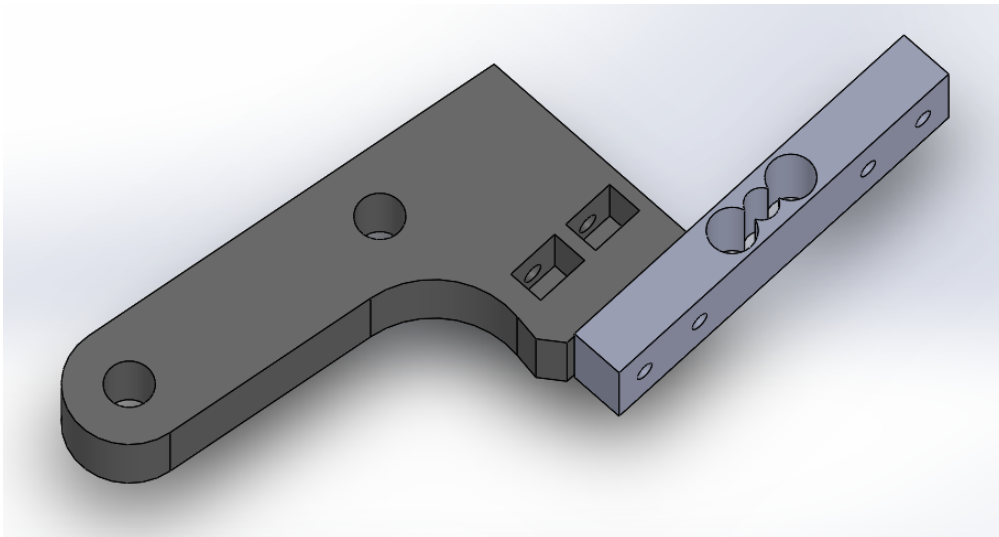Figure 3.1: Pre-model downloaded from the user-made library *grabcad.com*

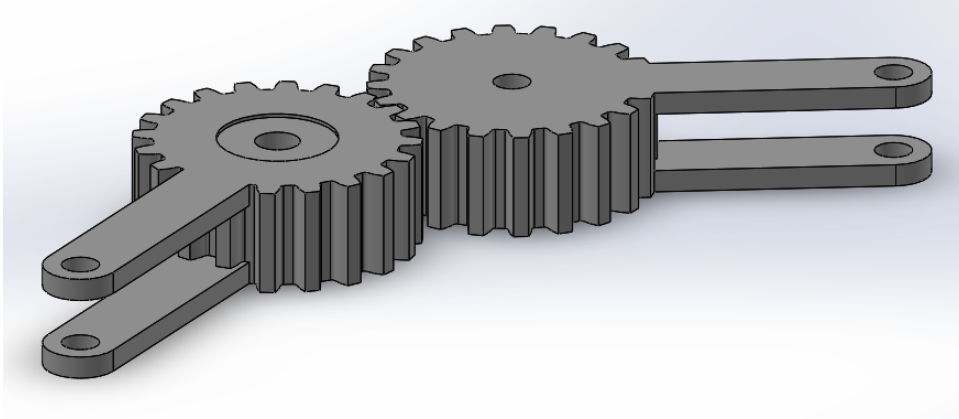Figure 3.2: Gripper phalanx adapted to fit load cell

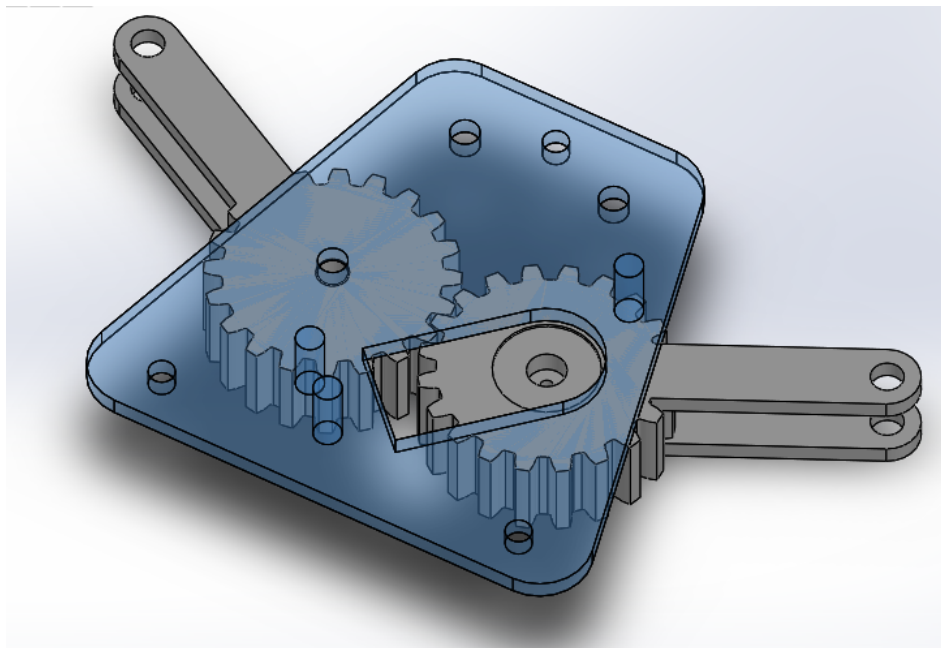Figure 3.3: Gear and rod structures unified into one piece

Figure 3.4: Top plate adapted to fit the servo motor

and GearMate. The Coincident mate forces two surfaces to be on the same plane but allows movement within the plane, it was used to make two pieces stay in touch with each other, as seen on figure 3.5. Concentric mate is used in circular shapes that are on parallel planes, it binds it's centers allowing only movement perpendicular to the plane. Together, Coincident and Concentric mates made possible the coupling of most pieces, as seen on figure 3.6. The only expected behaviour that required another mate was at the gears. As the project only uses motor in one of the gears, the movement had to be transmitted with the GearMate mate. This mate links two cylindrical faces so they will move around it's centers according to the ratio and transmission direction configured, as seen on figure 3.7.
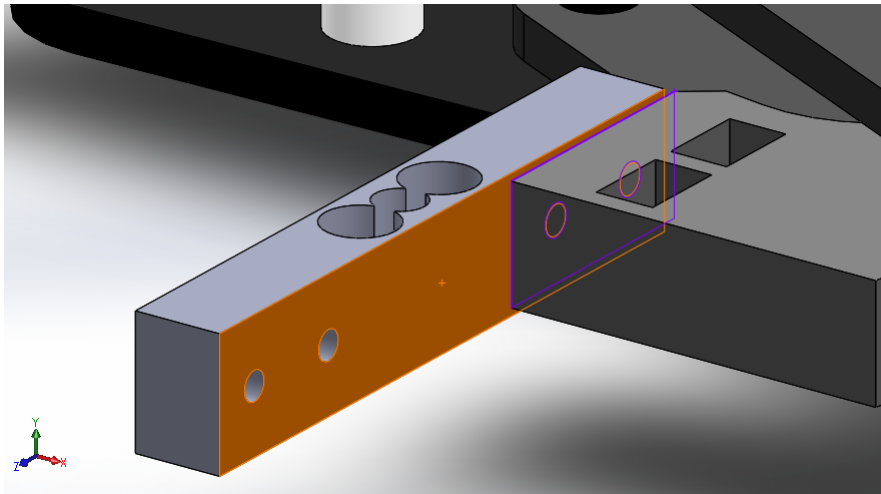
Figure 3.5: Coincident mate between the load cell and the phalanx

Following the assembly of the gripper pieces with all their relations, a motion study was made to evaluate how much power the servo motor should have in order to apply 0.5kgf on the grasped object. The simulation was made using the Motion Study feature of SolidWorks software.

The study consisted in two parts: configuring the motions and forces involved, and setting a sensor from which a torque graphic would be generated. About the forces configuration, each load cell had a force of 4.90332N applied to it's extremity, perpendicularly to the contact point's surface and towards opening the gripper, as seen on figure 3.8.
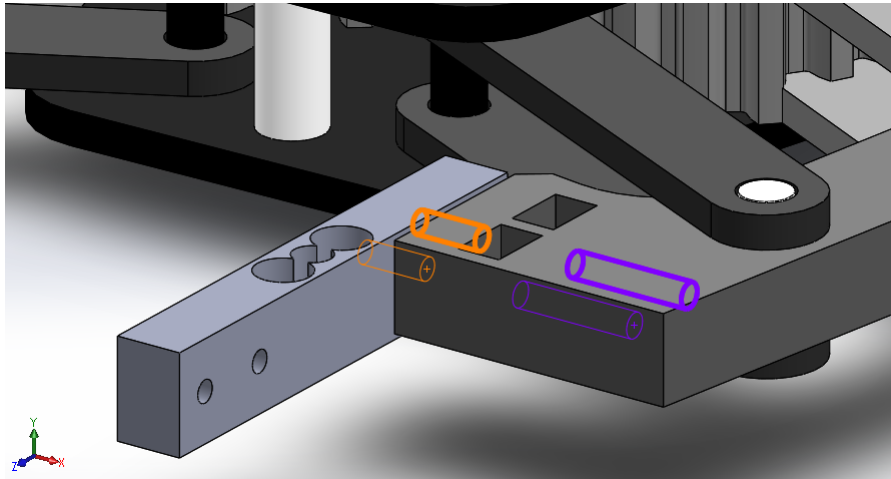
Figure 3.6: Concentric mate between the load cell and the phalanx
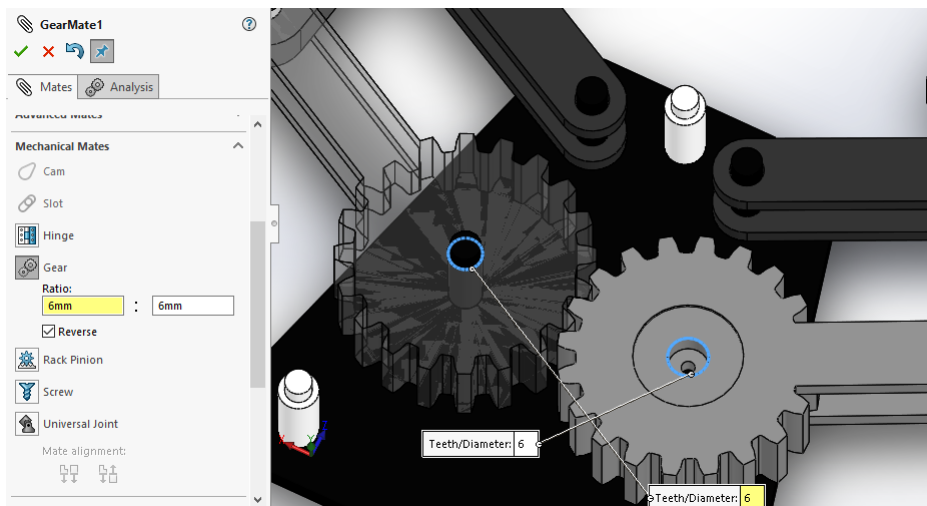
Figure 3.7: GearMate mate implemented on the two gears with the same ratio and reverse direction

The motion applied by the motor was simulated with the function RotaryMotor of the software. The movement was configured with the expression *STEP(TIME,0,0D,4,45D)*, that is characterized as a step, from 0 degrees to 45 degrees, initializing at the time 0s and completing it on time 4 seconds, the motion direction was towards closing the gripper, as shown on figure 3.9. Additionally, gravity force was also applied perpendicularly to the base.
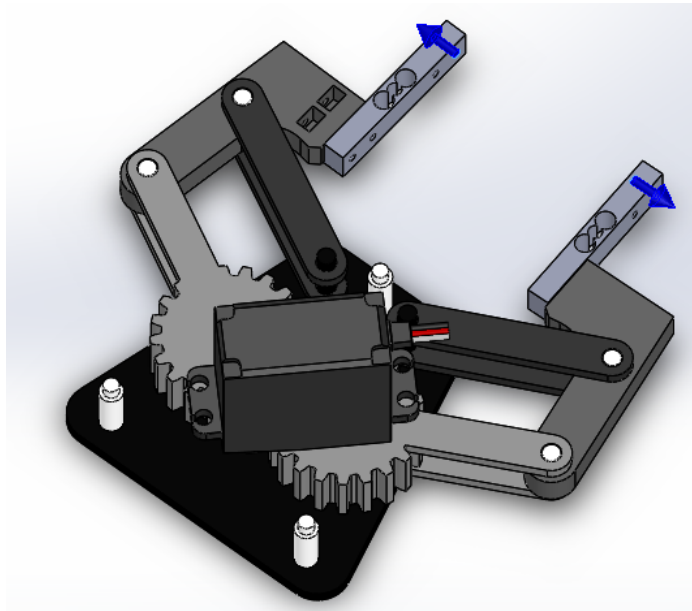
Figure 3.8: Forces implemented on Motion Study

SolidWorks Motion Study feature includes analysis of many different mechanical characteristics, such as stress, inertial properties, external forces, contacts, friction and torque studies. After setting up all the forces and motions involved on the study, a torque plot was configured.

The result of the study is shown on figure 3.10, and reveals that the toque increases as the angle between the force applied and the support rod connected to the gear tend towards perpendicularity. Also shows that the maximum value is on the positioning region the gripper will be when grasping an object, and that this value of torque was 409 *N.mm*, or 4.17 *kgf.cm*.

Figure 3.9: RotaryMotor implemented on Motion Study
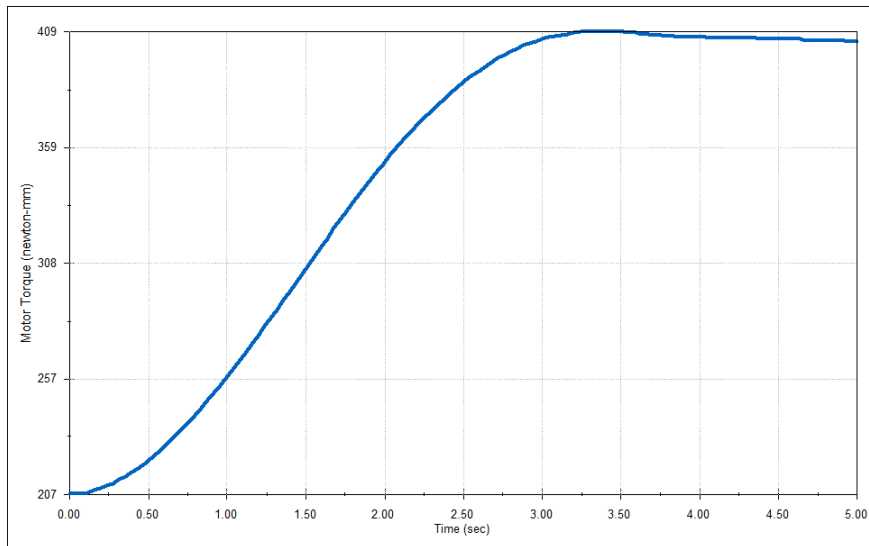
Figure 3.10: Torque chart generated by Motion Study

Chapter 4

Development

This chapter will approach the development of the study and it's implementation, it contains: a brief introduction to 3D printing and it's application on this project; the load cell functioning and the signal amplification circuit developed; an introduction to the NanoMDB interface used on the study; a brief introduction of LabVIEW and the control developed.

4.1 3D printing

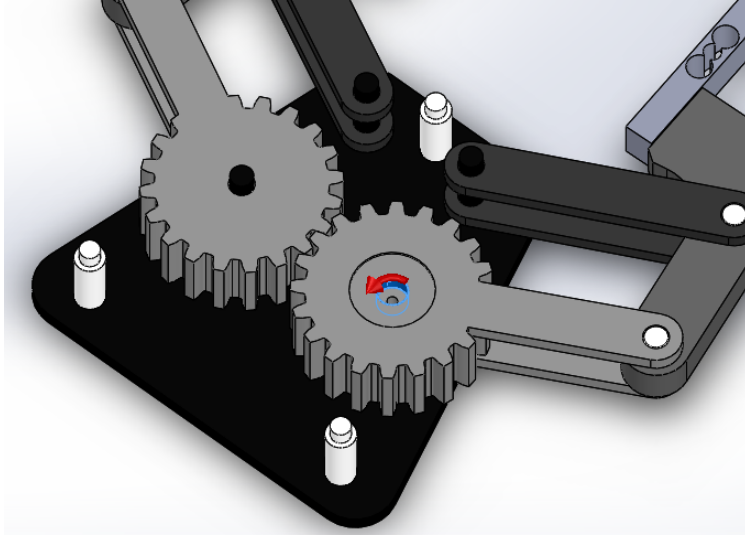The process of 3D printing consists on overlapping layers of material to form an object. The material is lied by the extruder, the part of the 3D printer responsible of heating and applying the material. After the modeling seen on the last chapter, each piece of the gripper was exported to .stl format, one of the most common formats for converting 3D CAD models into a representation of it's surface for stereolithography. The format is also know as Standard Triangle Language and Standard Tessellation Language. "The STL file format is generated using a tessellation process, which generates triangles to represent the CAD model, these triangles are described by a set of X, Y and Z coordinates for each of three vertices, and a unit normal vector to indicate which side of the triangle contains the mass." [7], an example of the file generated is seen on figure 4.1.

The pieces were printed with full fill in order to achieve maximum physical resistance
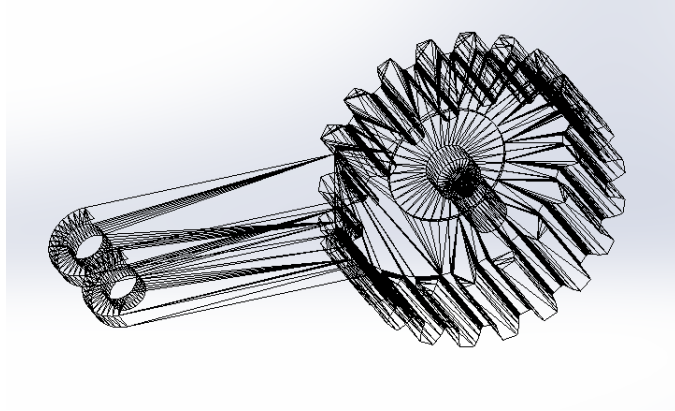
Figure 4.1: Visualization of piece generated on .stl format

and presented a good final result on most pieces, considering the scale of details some pieces required, as seen on figure 4.2.

Figure 4.2: Two identical

As the process involves overlapping malleable material, gravity and the printing orientation of the piece play an important role on the final result, as seen on figure 4.3.

The effect of gravity was observed when printing the gripper's phalanx. The piece was printed with it's larger surface facing up, and the outline of the piece had a good result, as

well as the holes for connecting with the pins from the rods. However, the holes designed to fit the bolts from the load cells did not present an acceptable result, requiring finishing. The piece was oriented in a way that the overlapping of materials was perpendicular to the center line of the cylindrical extrusion, resulting on the holes flattened.

Figure 4.3: Two identical cylinders printed at the same layer height in different orientations (left: vertically, right: horizontally) *3dhubs.com/knowledge-base/how-does-part-orientation-affect-3d-print/*

4.2   Signal acquisition

The load cell is a transducer, a measuring device that converts mechanical deformation into an electric resistance variation. The model used on this study is a single-point load cell. It contains four different strain gauges positioned around a metallic rod, as seen on figure 4.4. The four strain gauges are internally connected, forming a Wheatstone bridge.

Therefore, torsional strengths applied into the rod results on a variation on the resistances of the Wheatstone bridge. This unbalance of the resistance, along with a power supply, generates a potential difference between two terminals of the bridge, as seen on figure 4.5.

The sensor chosen had a considered linear behavior converting the strength applied into output signal, on the 100g to 550g range. That been said, the output signal has an amplitude on the order of millivolts, requiring an amplification circuit to be implemented.
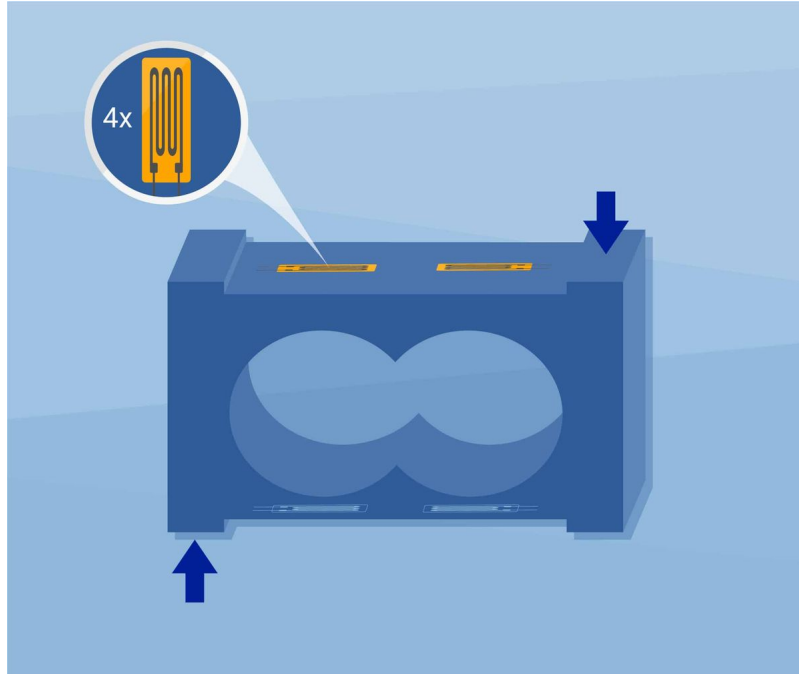
Figure 4.4: Model of a single-point load cell from *https://www.hbm.com/en/6768/what-is-a-load-cell-and-how-does-a-load-cell-work/*
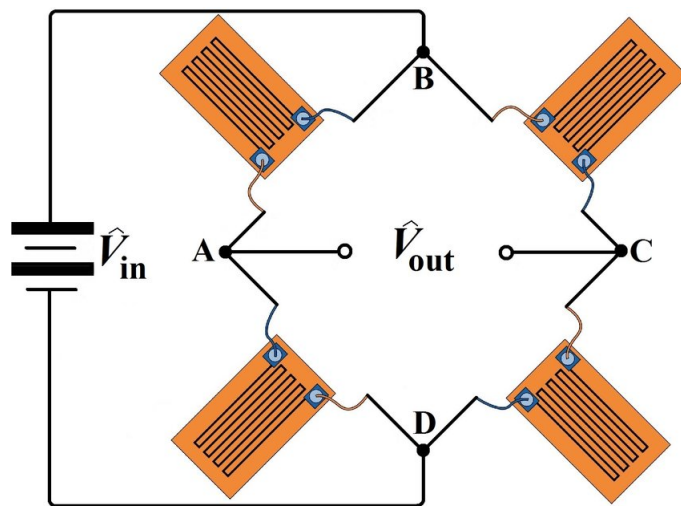

Figure 4.5: A full Wheatstone-bridge strain gauge circuit [8]

Due to lack of documentation of the chosen load cell, developing an amplifier circuit required empirically analysing the output signal when applying known forces with the support of a weighing-machine.

The original relation of input/output was approximately 0.008mV/g, achieving 3.8mV with 500g applied. The signal reading interface scale is from 0V to 5V, with a resolution of 4mV/bit. With this information a amplification circuit utilising an op-amp with positive feedback was designed.

The first step for designing the circuit was calculating the desired gain. Since there was no offset, the gain was calculated by dividing the interface scale, 0V to 5V, by the sensor scale, 0mV to 3.8mV, as seen on formula 4.1.

$$G = \frac{5 - 0}{0.0038 - 0} \approx 1315.789 \tag{4.1}$$

In order to smooth the gain, two op-amps were connected in series, dividing the total gain into two parcels. The formula that defines the op-amp gain at the positive feedback configuration is the following:

$$Vout = \frac{Rout + Rneg}{Rneg} \tag{4.2}$$

Due to the limitation of resistors commercial values, the chosen pair of resistors had the following values: Rout = $3.3k\Omega$, Rneg = 100Ω. Both op-amp were dimensioned equally, each with a gain of 34, as seen on formula 4.3, resulting on a total gain of 1156, as seen on formula 4.4.

$$Vout_1 = Vin * \frac{3.3k\Omega + 100\Omega}{100\Omega} = 34 * Vin \tag{4.3}$$

$$Vout_{total} = Vout_1 * \frac{3.3k\Omega + 100\Omega}{100\Omega} = 1156 * Vin \tag{4.4}$$

In addition to the amplifier operation, two capacitors were added as a high frequency filter in order to attenuate the noise from the signal input and amplification output. Also,

an over-voltage limiter sub circuit was implemented at the output of the amplifier to protect the analog input of the interface board. The protection sub circuit was composed of a 5.1V Zener diode and a $1k\Omega$ resistor to dissipate any voltage overload. The final acquisition circuit in seen in the figure 4.6.
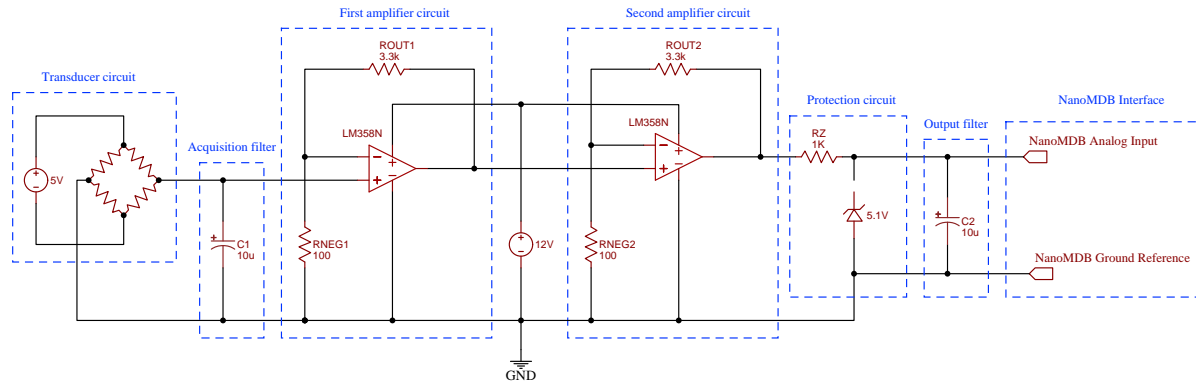

Figure 4.6: Signal acquisition circuit

4.3   Control system

The NanoMDB board is an Modbus Serial Communication Interface. It uses Arduino Nano as base hardware, attached to a shield and firmware developed by the company INFOCABO. This equipment was chosen for it's Modbus communication, for having a servo motor control signal configuration and for the support provided by professor Winderson dos Santos, who co-supervised this study and had experience with the device.

The shield allows easier access to the Arduino Nano pins, it also has two push-buttons connected to the digital inputs AI0 and AI1 and LED on the digital outputs for better visualization. The NanoMDB set contains 2 analog inputs with a 0V to 5V range, 4 digital inputs, 8 digital outputs and 2 PWM outputs, as seen on figure 4.7. All the digital outputs can also be configured as servo motors control signal. The board also has 2 native PID controllers internally connected to the PWM outputs. All the interaction and configuration between LabVIEW and the board is made by assigning values to coils

addresses on the Modbus protocol. The firmware running on the NanoMDB is intellectual property of the company INFOCABO.
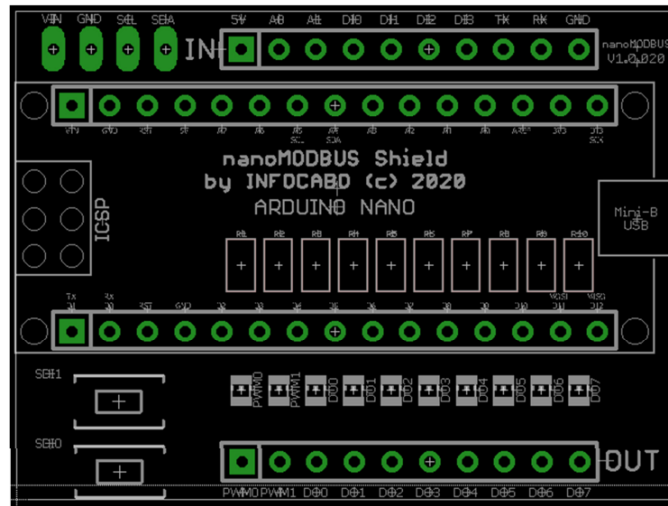

Figure 4.7: NanoMDB pinout

LabVIEW is an acronym for Laboratory Virtual Instrument Engineering Workbench, an environment for visual programming. As said by National Instruments, maintainer of LabVIEW, in their official website: "LabVIEW is systems engineering software for applications that require test, measurement, and control with rapid access to hardware and data insights".

The LabVIEW software was chosen for it's wide library options, including a Modbus Serial communication protocol. Also, for it's panel visualization, allowing an easy supervision of the variables involved on the process.

The block diagram can be divided as follows: initialization, variable reading, control network, output treatment and coil writing. This steps are all inside a while loop, except for the initialization, as seen on figure 4.8.

The initialization step consists on the creation of the Modbus Serial Master instance and the baud rate (communication speed) configuration, COM port selection, Modbus network address, parity and the type of serial transmission data unit selection. There's also a scale conversion definition block, as seen on figure 4.9.

The variable reading step has a Read Input Registers block, responsible for acquiring
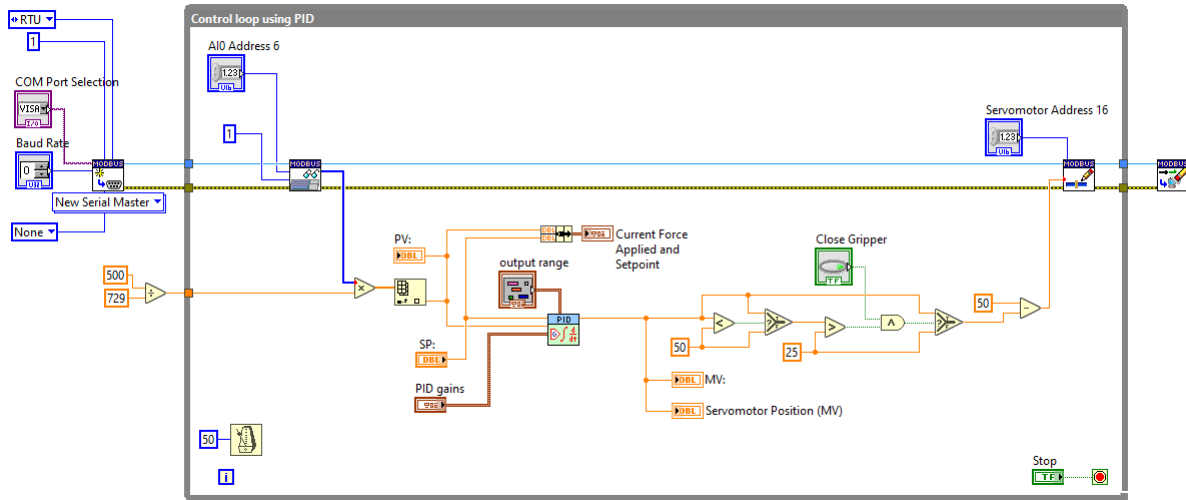
Figure 4.8: LabVIEW control block diagram
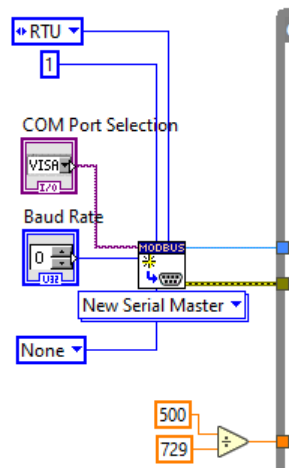
Figure 4.9: LabVIEW initialization step block diagram

the NanoMDB analog input value, which is connected to the output of the load cell signal amplification circuit. It contains a scale adjustment block that converts the analog reading to the 0g to 500g range, used on the control step, as shown on figure 4.10.
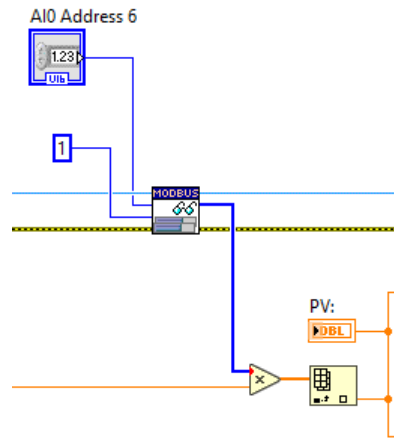
Figure 4.10: LabVIEW variable reading step block diagram

The control network step consists on a PID loop responsible for controlling the position, seen on figure 4.11, and direction of the gripper, it also has indicator referenced on the panel, figure 4.12.
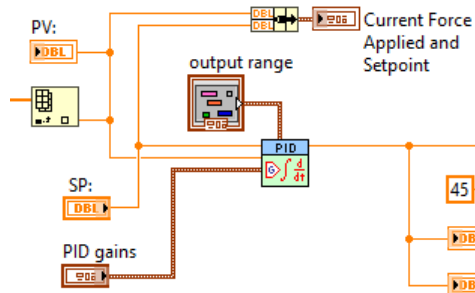
Figure 4.11: LabVIEW control network step block diagram

The output treatment (figure 4.13) aims to prevent that the control network output overpasses the physical movement limitation of the gripper.

The writing step has a Write Single Holding Register block that assigns the signal from the treatment step into the Modbus address defined as the servo motor position control, as seen on figure 4.14.

31

Figure 4.12: LabVIEW panel design
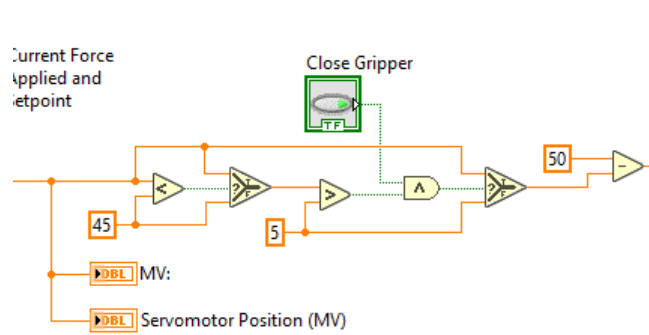
Figure 4.13: LabVIEW control network step block diagram
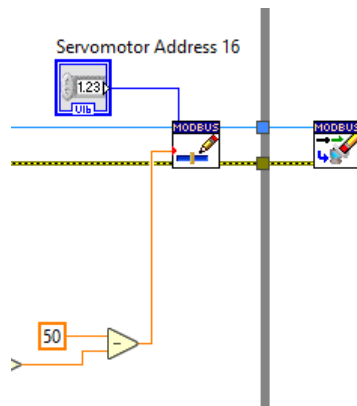
Figure 4.14: LabVIEW control network step block diagram

4.4   Implementation difficulties

The implementation process had some unforeseen obstacles. One of the issues was related to the subject presented on the section 4.1, the other was a sum of load cell construction characteristics and manipulation.
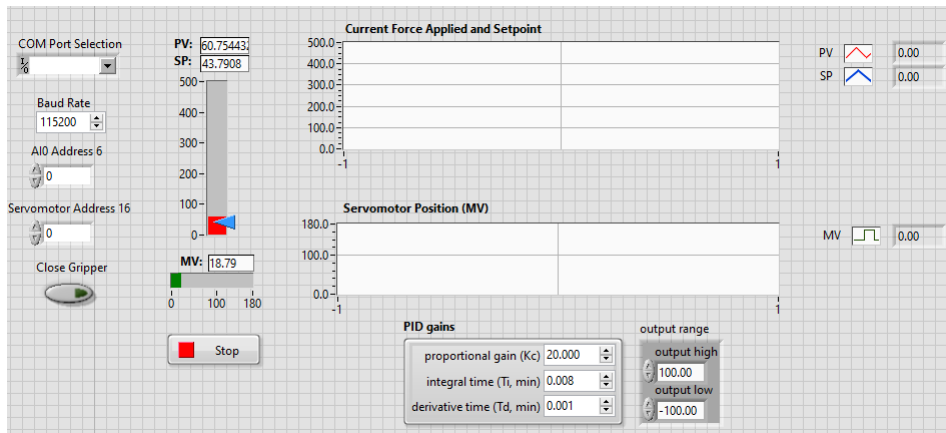
As the phalanx were printed with the bolt holes normal vector parallel to the horizontal plane, the final result of the hole was distorted on the top half. In order to fix it, a small drill was used. The friction between the drill and the piece caused a material overheating, melting and deforming the plastic, requiring a new and more careful finishing, but preventing the nuts to fit.

The load cell had a extremely thin and fragile wiring, the first attempt to improve it's resistance was wrapping the wires with heat shrinkable tube and welding a more resistant extension wire set. Unfortunately, the process of wrapping did not protect the section of wires close to the load cell body and during manipulation one of the wires snapped, making one of the load cells unusable. From this, the need of reinforcement on this section was perceived, so epoxy resin was applied to the second load cell.

Chapter 5

Tests and discussion

This chapter will describe the tests and evaluations made during the prototyping and assemble of the gripper. It also contains the results, identified problems and probable causes.

5.1   Load cell

The first test made was to estimate the output amplitude of the load cell with 500gf applied in order to design the amplification circuit to fully use the input range of the NanoMDB, as describer on the last chapter.

The first amplification circuit developed has a single step amplification, utilizing one op-amp for each load cell. The circuit was designed with a pair of commercial resistors $Rout = 130k\Omega, Rneg = 100\Omega$ (figure 5.1), resulting on a theoretical gain of 1301. The output result, though, was bellow the expected, achieving only 52% of the designed gain, about 2.50V.

It was assumed that the voltage gap was due to an excessively large gain for the op-amp to perform in one step. Once one of the load cells had been compromised and the amplification circuit should be revised, it was decided to divide the gain evenly by the two available op-amps. The pair of gains chosen was the one that came closest, using commercial resistors, to the square root of the originally designed gain, resulting in a
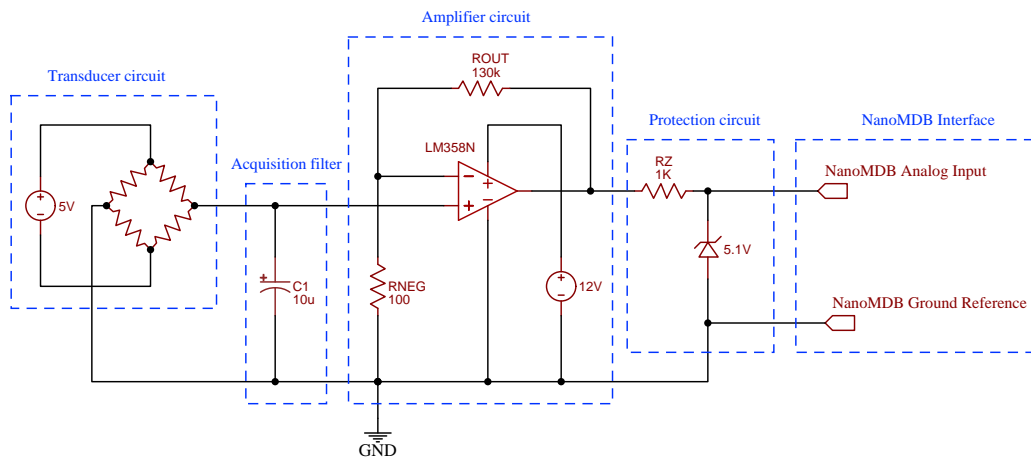
Figure 5.1: First design of signal acquisition circuit

cascade gain of G = 34 * 34 = 1156, as shown in the previous chapter.

Known weights, assessed by a weighing-machine, were suspended perpendicularly to the load cell, in order to emulate the the force application force of the gripper. A series of measurements of the acquisition set were made to evaluate it's response to force application. The results are presented on the graph figures 5.2 and 5.3.
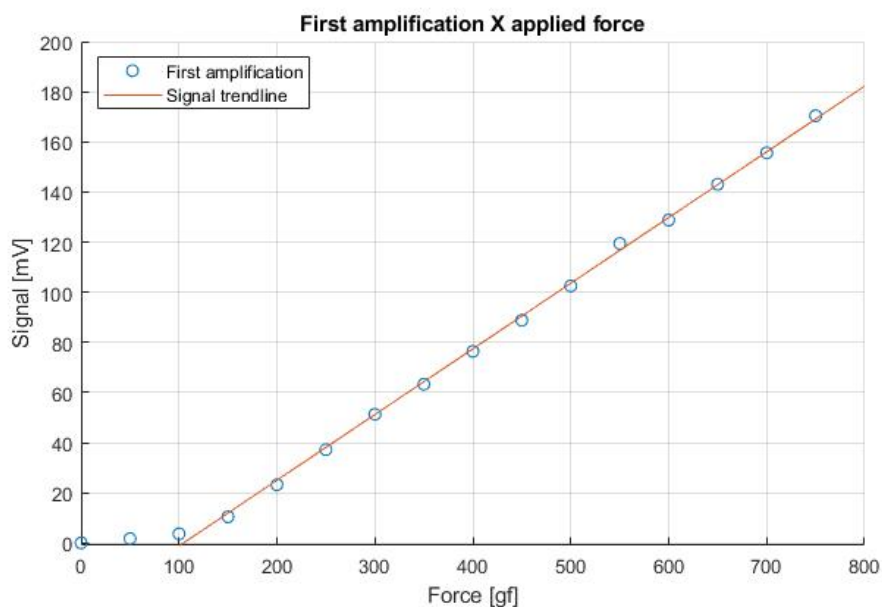
Figure 5.2: First amplification signal response to applied force

The data collected on the first amplification show that the load cell presents a considered linear response starting from 100gf, bellow this value the sensor presented a behavior that did not follow the trend of the curve. Disregarding the first two points, a trend line was calculated that follows the equation 0.262 * x -27.4.
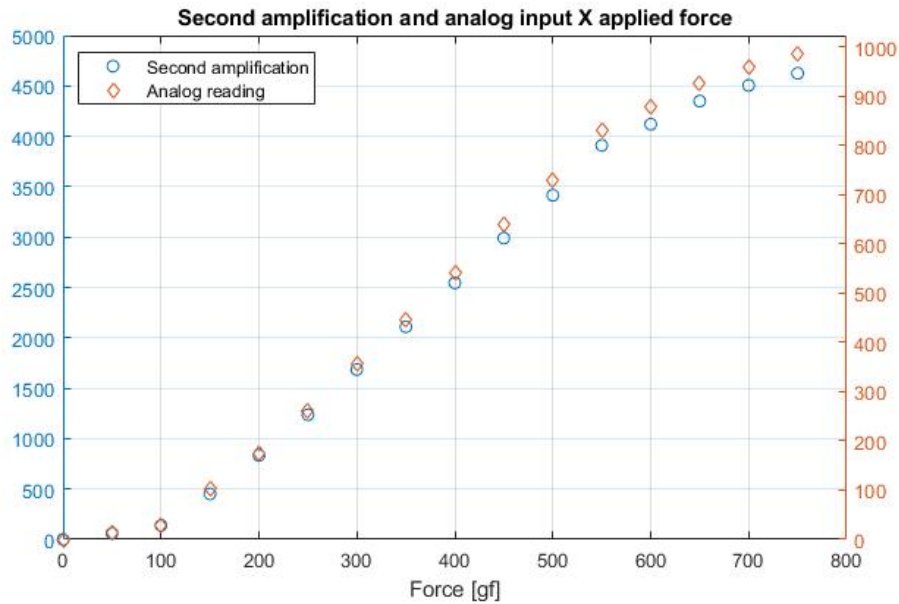
Figure 5.3: Second amplification signal [mV] and analog input reading [bit] response to applied force

As expected, the second amplification signal and the NanoMDB analog input reading presented the linearity starting from the same point on the graph, but it is noted that, when reaching 600gf, the amplification circuit starts to saturate, result of the voltage source limitation, as seen on figure 5.3. It is also noted that the total gain did no reach the designed value, achieving 74% of the amplitude. This loss can be related to three main factors: losses inherent to the amplification circuit, imprecision of the values of the resistors used and imprecision of the estimated maximum value of the load cell output signal, due to the use of an ordinary multimeter to measure a low amplitude voltages. Despite the discrepancy between the expected value and the real value, the amplification proved to be sufficient for the range of forces proposed in this work.

5.2   Servo motor

In order to observe the internal positioning reference of the motor to set the ascending or descending direction of the control, a servo motor movement test was performed. The test was also for determining the physical movement limitation of the gripper. The positioning was made through direct commands made on the modbus addresses of the NanoMDB interface, through the LabVIEW Modbus Serial connection library. During these tests, it was seen that only the fitting of the motor shaft in the gear hole had sufficient mechanical adherence to move the entire structure, but it did slip with any greater resistance found. Therefore, this coupling was used only for reference positioning tests.

Once the acquisition circuit was finished and it's manipulation was no longer necessary, the load cell was permanently fixated with bolts as support and epoxi resin for fixating on the gripper. The original fixation with bolts and nuts was not possible because of the 3D printing problems described on chapter 4.

The servo motor shaft, was permanently fixed to the gear with instant glue, in order to prevent slipping during the application of force, as noted in the first tests. After fixating all parts, tests were made to define the PID gains of the control system. As an immediate result, it was noted that the engine was not able to apply the expected force, despite the calculation of the required motor torque. The first equipment ordered was damaged and was replaced by the supplier with a supposedly similar model, but without identification or datasheet. This motor, after fixed, applied a maximum force of only 83gf in steady state at the tip of the actuator.

5.3   PID Controller

Although the servo motor caused a big limitation to the control range of the system, it was sufficient to test the operation of the command and control software implemented in LabVIEW and tune the PID controller.

In order to test the functionality of the implemented solution, the setpoint for applied

force was set to 50gf, value chosen for having a good reading range and for not operation on the saturation zone of the motor.

The PID manual tuning was made as a iterative process where each gain was individually adjusted to achieve the desired control response. The first gain set was the proportional gain (Kc), responsible for the response speed of the controller. Once the Kc reached a satisfactory value, the next parameter adjusted was the integral time (Ti), this parcel of the controller actuation is responsible for attenuating the steady-state error. The next in order was the derivative time, this variable is responsible for holding back sudden drastic shifts on the controller manipulated variable.

The values found on one iteration of the process were used as starting point to the next adjustment loop. The process was repeated multiple times until the parameters were tuned individually and together. Figure 5.4 contains one of the first runs on the adjustment loop. As noticed, the controller had a fast response but the proportional gain was too high resulting on a oscillating system.

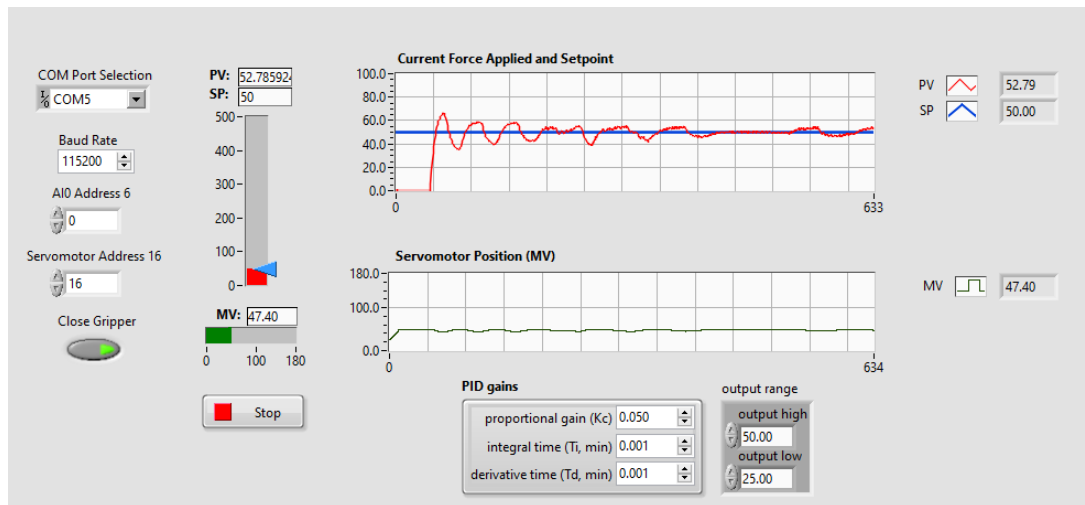Figure 5.4: PID response to Kc = 0.050; Ti = 0.001; Td = 0.001

After some iterations, the final set of gains were defined. Figure 5.5 shows the control actuation and the response of the process variable. The control of the overshoot is a critical point when designing a controlled force gripper, since it's applications are usually related to grasping delicate objects, and any over-pressure may damage the grasped piece.

On the process variable graph it is noted that the application of force increases smoothly towards the setpoint and presents a overshoot of 10%, which is acceptable on this study's scope.
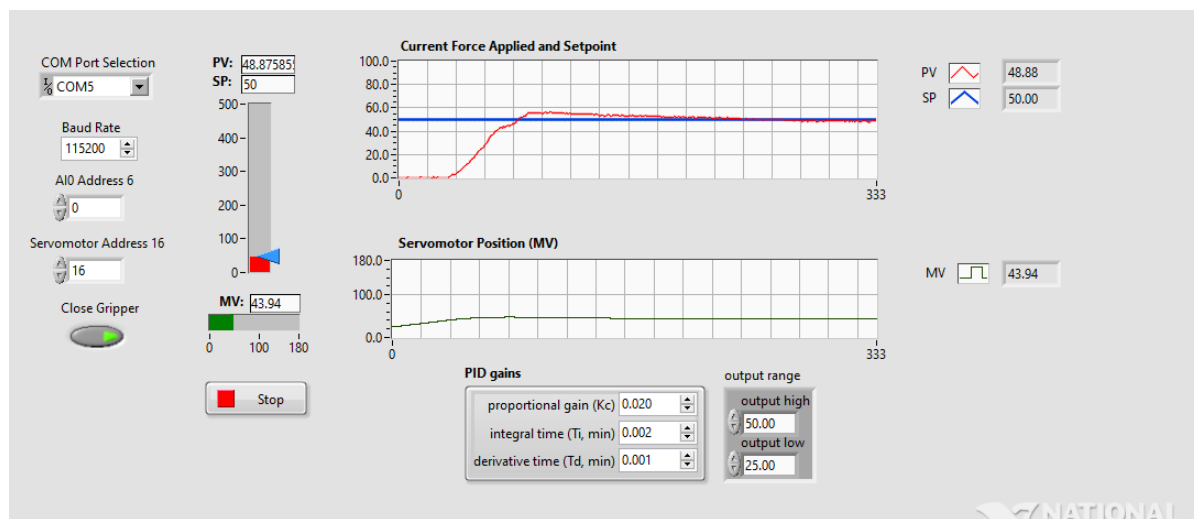

Figure 5.5: PID response to final set of parameters

Chapter 6

Conclusions

The final considerations of this study will contain an analysis of fulfillment of the objectives and specifications proposed on chapter 1, the knowledge acquired during the study and future work suggestions.

6.1 Objectives analysis

The design of the gripper with the software SolidWorks was presented on chapter 3 and showed the modelling and motion study used to calculate the torque needed by the servo motor in order to apply the specified force, as well as the development of the models for 3D printing. The production and assemble of the pieces were, along with the implementation difficulties, described on chapter 4. Apart from some 3D printing imprecision and unexpected servo motor behavior, the design and final result of the gripper structure were as expected.

The control system, including the acquisition hardware, communication hardware and LabVIEW software had, as major issue, the physical fragility of the load cell wiring. This constructive characteristic, resulted on implementation delays and required rework and adapting. Another obstacle was the poor estimation from the load cell signal amplitude, resulting on a incorrect amplification project gain. Nevertheless, the control system was implemented and operated successfully, despite the changes in range and precision of the

41

reading.

As to the specifications of the project, the gripper had a servo motor electric actuation; the final force applied by the tool was below the proposed on this study, but was still controlled and limited. The final result, despite the errors, allowed a study of the applied force control by manipulating a servo motor positioning.

6.2   Future work suggestions

As suggestion for future studies is the implementation of a larger scale gripper, with a more resistant structure and stronger servo motor. Another suggestion is developing a similar study replacing the servo motor for a DC motor. A last suggestion is studying the relation between the applied force and the current drained by the motor.

Bibliography

[1] M. Ceccarelli, "Notes for a history of grasping devices", in *Grasping in Robotics*, G. Carbone, Ed., 1st, London, England: Springer-Verlag London, 2013, ISBN: 978-1-4471-4663-6.

[2] P. O. Hugo, "Industrial grippers: State-of-the-art and main design characteristics", in *Grasping in Robotics*, G. Carbone, Ed., 1st, London, England: Springer-Verlag London, 2013, ISBN: 978-1-4471-4663-6.

[3] N. R. Sinatra, C. B. Teeple, D. M. Vogt, K. K. Parker, D. F. Gruber, and R. J. Wood, "Ultragentle manipulation of delicate structures using a soft robotic gripper", *Science Robotics*, vol. 4, no. 33, 2019. DOI: `10.1126/scirobotics.aax5425`. eprint: `https://robotics.sciencemag.org/content/4/33/eaax5425.full.pdf`. [Online]. Available: `https://robotics.sciencemag.org/content/4/33/eaax5425`.

[4] R. Arumathanthri, B. Abeygoonawardana, I. Kumarasinghe, D. Chathuranga, T. Lalitharatne, and A. Kulasekera, "A soft robotic gripper with sensory feedback fabricated by latex using coagulant dipping process", Dec. 2018, pp. 2082–2087. DOI: `10.1109/ROBIO.2018.8665091`.

[5] K. Hermann, R. Hostettler, M. Zimmermann, and A. V. Sureshbabu, "A joint-selective robotic gripper with actuation mode switching", in *2019 IEEE 15th International Conference on Automation Science and Engineering (CASE)*, Aug. 2019, pp. 1532–1539. DOI: `10.1109/COASE.2019.8842987`.

[6] A. Milojević, M. Tomić, H. Handroos, and Ž. Ćojbašić, "Novel smart and compliant robotic gripper: Design, modelling, experiments and control", in *IEEE EUROCON*

2019 -18th International Conference on Smart Technologies, Jul. 2019, pp. 1–6. DOI: `10.1109/EUROCON.2019.8861561`.

[7] M. Eragubi, "Slicing 3d cad model in stl format and laser path generation", *International Journal of Innovation, Management and Technology*, vol. 4, 2013. DOI: `10.7763/ijimt.2013.v4.431`. (visited on 04/24/2020).

[8] H. Akbari and A. Kazerooni, "Improving the coupling errors of a maltese cross-beams type six-axis force/moment sensor using numerical shape-optimization technique", *Measurement*, vol. 126, pp. 342–355, May 2018. DOI: `10.1016/j.measurement.2018.05.074`.